Supporting Information

A self-powered porous ZnS/PVDF-HFP mechanoluminescent composite film that converts human movement into eye-readable light

Haitao Lia, Yihe Zhanga, Han Daib, Wangshu Tonga, Yan Zhoua, Junfeng Zhaoc, and Qi Ana**

[a]Beijing Key Laboratory of Materials Utilization of Nonmetallic Minerals and Solid Wastes, National Laboratory of Mineral Materials, School of Materials Science and Technology, China University of Geosciences, Beijing, 100083, China.

[b]Department of materials, School of Technology, Yantai Nanshan University, Longkou, Shandong Province, 265713 (China)

[c]Institute of theoretical chemistry, Jilin University, Changchun, Jilin Province, 130023 (China)

Section S1. Material.

PVDF-HFP (density 1.78 g cm^{-3}, 5-20% molar of hexafluoropropene) was purchased from Sigma-Aldrich. N,N-dimethyl formamide (DMF, 99.5%) were obtained from local commercial sources and used as received. Mental-doped ZnSandethylene-vinyl acetate copolymer(EVA) were purchased from Ou Bai Te Technology Co. Ltd., Shenzhen.

Section S2. The calculation of β phase fraction in PVDF-HFP and the calculation of porosity.

The β-phase fractions were calculated via the area of the vibrational bands of the α and β phases in FTIR according to formula (S1).[1]

$$F(\beta) = \frac{X_\beta}{X_\alpha + X_\beta} = \frac{A_\beta}{1.26A_\alpha + A_\beta} \quad \text{(S1)}$$

Where X_α and X_β are the crystalline mass fractions of the α and β phases, respectively, and $A_\alpha$and $A_\beta$are their peak intensities at 764 and 840 cm^{-1}. The 1.26 factor accounts for the ratio in the absorption coefficients at 764 and 840 cm^{-1}.

The porosity can be calculated by following formula (S2).

$$P = \frac{V_0 - V}{V_0} \times 100\% \quad \text{(S2)}$$

Where P is porosity, V_0 is the volume of the porous films that can be measured by drainage method, V is the absolute volume of the solid PVDF-HFP films can be calculated by actual density of materials (1798 kg/m^3).

Section S3. The calculation of hydrogen bond between ZnS and PVDF-HFP.

All the geometries and vibrational frequencies of the stationary points involved in the complex of ZnS and $CH_3CF_2CF_3$ were calculated without constraints using M06-2X functional[2,3], 6-311+G(d,p) basis set[6] for the C, H and F atoms, and the SDD basis set[5] for Zn and S atoms (the M06-2X/6-311+G(d,p)~SDD level). Frequency calculations at the same level of theory have also been performed to identify all of the stationary points as minima (zero imaginary frequencies), and to provide the vibrational motions. All calculations were performed via the Gaussian 09 program package.[6]

In the complex **P** formed by ZnS and **R** (Figure 1), The bond distance of S···H was 2.244 Å (Table S1), indicating a strong interaction between sulfur and hydrogen atoms.[7] This interaction leads to obvious frequency shifts of the stretching vibration of the C-H and C-F chemical bonds, shown in Table S2.

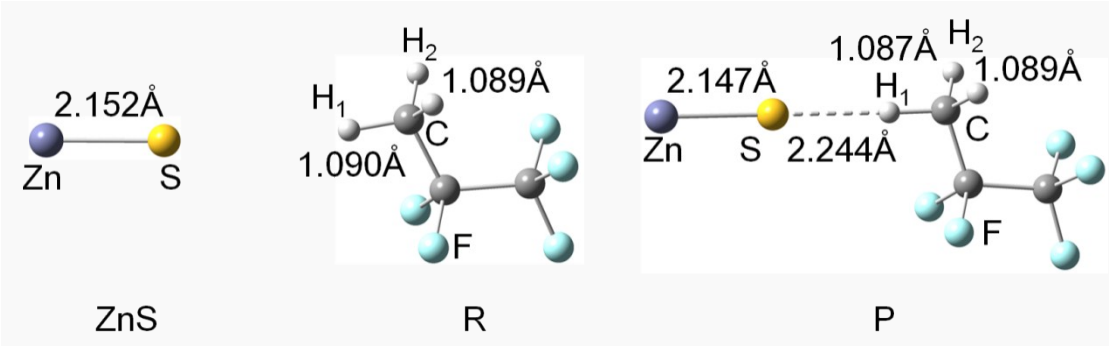

Figure S1. Key ground-state structures involved in the reactions of the reactant ZnS with $CH_3CF_2CF_3$ at the M062X level of theory.

Table S1: Geometric parameters of stationary points in the reactions of ZnS with $CH_3CF_2CF_3$ calculated at the M062X/6-311+G(d,p) level of theory. Bond length, [Å].

	R_{Zn-S}	R_{C-H1}	R_{C-H2}	R_{S-H1}
ZnS	2.152			
R		1.090	1.089	
P	2.147	1.087	1.089	2.244

Table S2. Stretching vibration of CH_3 [$\nu_s(CH_3)$] and asymmetrical stretching vibration of CF_2 [$\nu_{as}(CF_2)$]. Vibrational frequency, [cm^{-1}].

	$\nu_s(CH_3)$	$\nu_{as}(CF_2)$
R	3089.86	1245.13
P	3087.09	1247.10

Section S4. Blue shift of asymmetric stretching vibration of F-C-F from ZnS/PVDF-HFP.

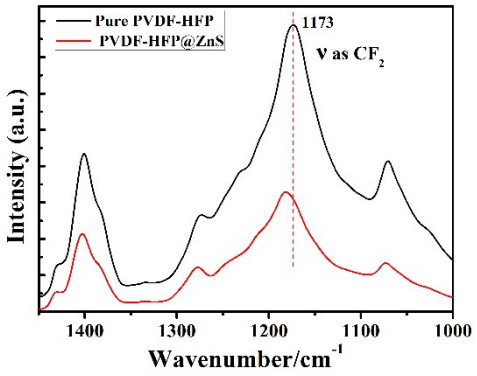

Figure S2 FTIR spectra in the region 1400-1000 cm^{-1} for ZnS/PVDF-HFP composite.

Section S5. The XPS peak analysis of PVDF-HPF and ZnS/PVDF-HPF.

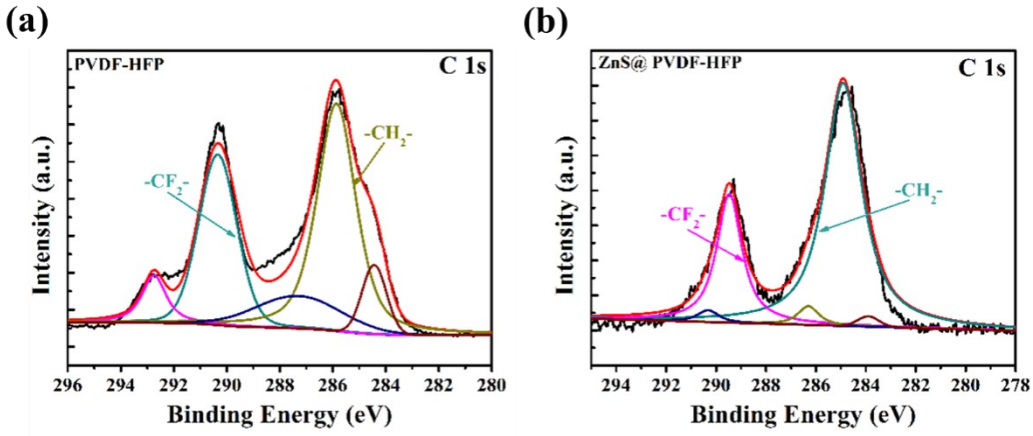

Figure S3 C 1s core-level spectra of (a) pure PVDF-HFP and (b) ZnS/PVDF-HFP.

In the case of the PVDF-HFP (FigS3 a), the C1s core-level spectrum was curve-fitted with five peak components, where the CH_2 and CF_2 peaks appear at 285.9 and 290.4 eV, respectively. The components with BE at 284.4, 287.3, and 292.8 eV were attributed.to C–C/C–H, CF, and CF_3 species, respectively, of the copolymerized HFP chain.[8] In XPS spectra of ZnS@PVDF-HFP, the CH_2 and CF_2 peaks appeared at 284.9 and 289.5 eV respectively. Compared with pure PVDF-HFP,

these peaks were shifted to lower binding energy values, indicating that PVDF-HFP received electrons in the composite.

Section S6. The characterization of power generation for ZnS/PVDF-HFP, and The comparison of piezoelectric properties between PVDF-HFP with porous and PVDF-HFP without porous.

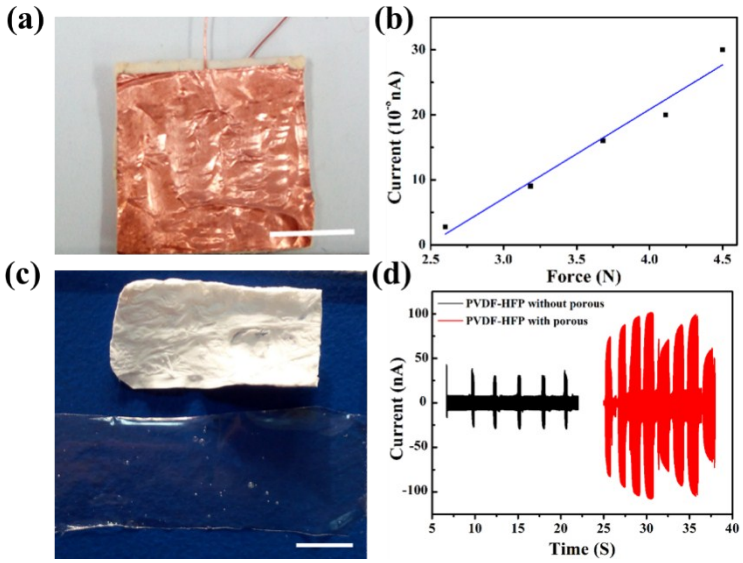

Figure S4 a) The digital photo of the piezoelectric measurement of the ZnS/PVDF-HFP composite film, wrapped in copper foil and connected to the electrochemical station by copper wires. b) The linear relationship between piezoelectric current and the magnitude of the applied forces 2.60, 3.18, 3.68, 4.11, 4.50N(generated by a plastic ball of 6 g fell from the different height).c) The optical photograph of PVDF-HFP with porous (up, the mass is about 0.04g) and PVDF-HFP without porous (down, the mass is about 0.04g).d) The comparison of piezoelectric properties generated under finger tapping between PVDF-HFP with porous and PVDF-HFP without porous. The scale bar correspond to 0.5 cm.

Section S7.TGA curves for pristine PVDF-HFP and ZnS/ PVDF-HFP.

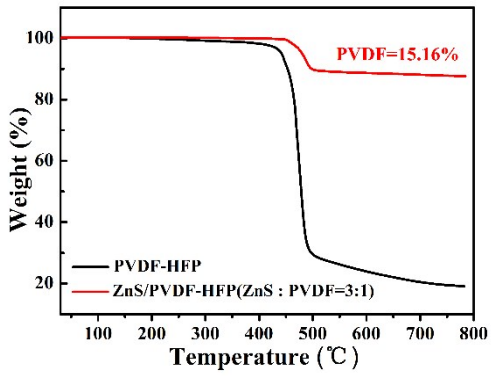

Figure S5 TGA curves for pristine PVDF-HFP and ZnS/ PVDF-HFP at a heating rate of $10^{\circ}C \cdot min^{-1}$ in a nitrogen atmosphere. The results show that the fraction of PVDF-HFP in ZnS/ PVDF-HFP composite (ZnS:PVDF-HFP= 3:1) is about 15.16%.

Section S8. SEM image of the different mental-doped ZnS particles.

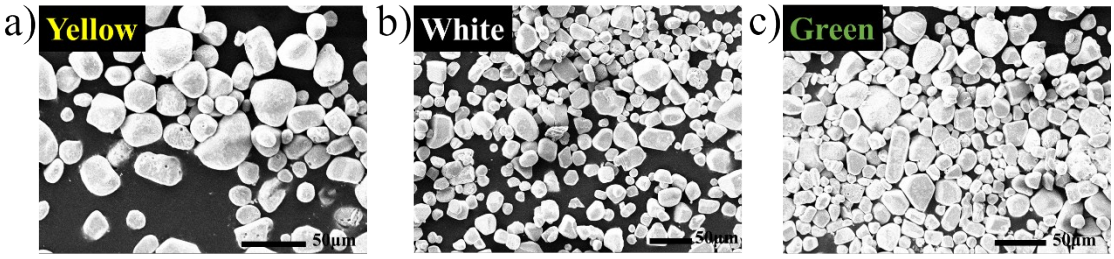

Figure S6 SEM image of the doped ZnS particles. The samples in (a, b, c) generate yellow, white, and green light.

Section S9. Information displaying under low frequency body movements

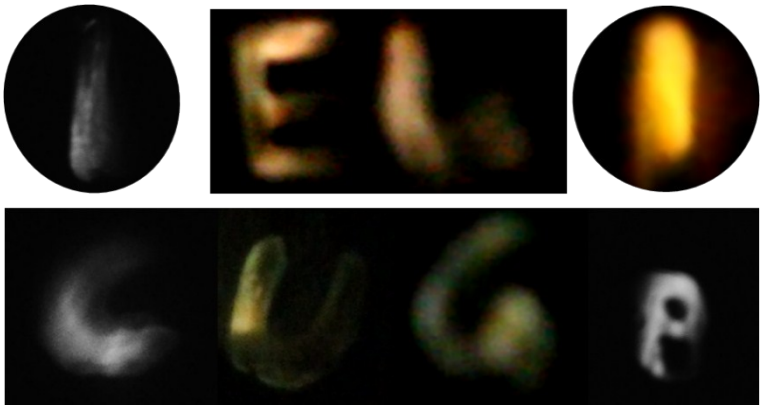

Figure S7 The illuminating pattern generated by finger rubbings of Arabic number "**1**" and letters"**EL**" and "**CUGB**".

Section S10. The luminescent intensities of different values of external forces.

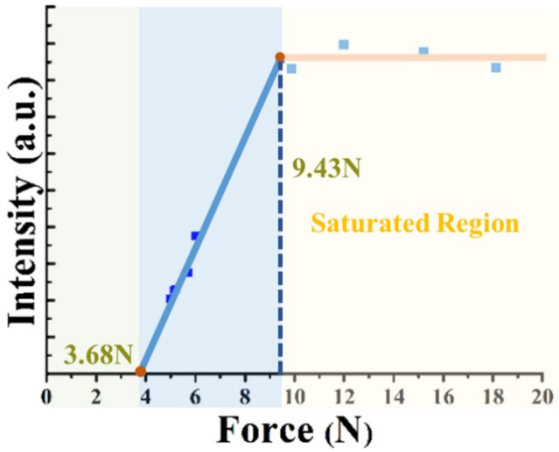

Figure S8 The luminescent intensities of different values of external forces.

There has two critical points for the optimized luminescent. From the Fig. S8, we can see that the luminescence could not be produced when the loading force is below 3.68N, because of the insufficiency of electric field intensity. While the responding intensity of luminescence will reach saturation when such force is over 9.43N. It may be hard to reach such force during the saturated area for some body movement such as finger movement.

Section S11. The influence of the size effect of porous on luminescence.

Table S3 Summary of experimental conditions (1g PVDF in different volume DMF) and porous film physical properties including pore diameter (D), standard deviation (SD), film porosity (P).

DMF(mL)	D(μm)	SD	P
4	0.81	0.02070	36.24%
8	1.10	0.04860	61.00%
16	3.27	0.10242	87.97%

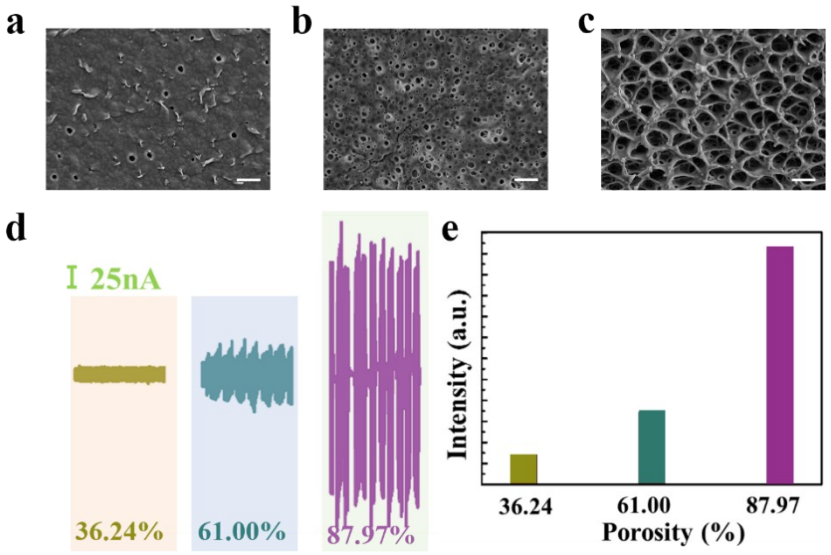

Figure S9 The SEM image of the porous PVDF-HFP film prepared at different DMF volume. a) 1g PVDF-HFP in 4mL DMF, b) 1g PVDF-HFP in 8mL DMF, c) 1g PVDF-HFP in 16mL DMF. d) The piezoelectric current and c) the luminescent intensities of different porosity films under the same values of external forces. (The scale bar represents 4μm.)

References

[1] Jr. R. Gregorio and M. Cestari, *J. Polym. Sci., Part B: Polym. Phys.* 1994, **32**, 859.

[2] Y. Zhao and D.Truhlar, *J. Chem. Phys.* 2006, **125**, 194101.

[3] Y. Zhao and D. Truhlar, *Theor. Chem. Acc.* 2008, **120**, 215.

[4] M. P. Andersson and P. Uvdal, *J. Phys. Chem. A* 2005, **109**, 2937.

[5] X. Cao and M. Dolg, *J. Mol. Struct.: THEOCHEM* 2002 , **581**, 139.

[6] M. J. Frisch, G. W. Trucks, H. B. Schlegel, G. E. Scuseria, M. A. Robb, J. R. Cheeseman, G. Scalmani, V. Barone, B. Mennucci, G. A. Petersson, H. Nakatsuji, M. Caricato, X. Li, H. P. Hratchian, A. F. Izmaylov, J. Bloino, G. Zheng, J. L. Sonnenberg, M. Hada, M. Ehara, K. Toyota, R. Fukuda, J. Hasegawa, M. Ishida, T. Nakajima, Y. Honda, O. Kitao, H. Nakai, T. Vreven, J. A. Montgomery, Jr., J. E. Peralta, F. Ogliaro, M. Bearpark, J. J. Heyd, E. Brothers, K. N. Kudin, V. N. Staroverov, T. Keith, R. Kobayashi, J. Normand, K. Raghavachari, A. Rendell, J. C. Burant, S. S. Iyengar, J. Tomasi, M. Cossi, N. Rega, J. M. Millam, M. Klene, J. E. Knox, J. B. Cross, V. Bakken, C. Adamo, J. Jaramillo, R. Gomperts, R. E. Stratmann, O. Yazyev, A. J. Austin, R. Cammi, C. Pomelli, J. W. Ochterski, R. L. Martin, K. Morokuma, V. G. Zakrzewski, G. A. Voth, P.

Salvador, J. J. Dannenberg, S. Dapprich, A. D. Daniels, O. Farkas, J. B. Foresman, J. V. Ortiz, J. Cioslowski, and D. J. Fox, Gaussian 09, Revision E.01.(Gaussian, Inc., Wallingford CT, 2013).

[7] H. S. Biswal and P. R. Shirhatti, *J. Phys. Chem. A* 2009, **113** , 5633.

[8] S. Mitra, A. Ghanbari-Siahkalia, P. Kingshott, K. Almdal, H. K. Rehmeier and A. G. Christensen, *Polym. Degrad. Stab.* 2004 , **83**, 195.